

Recent Developments in Through-Process Modelling of Aluminium Die-Castings

Cato Dørum^{1,2}, Hans Ivar Laukli^{2,3}, Odd Sture Hopperstad^{2,4}, Torodd Berstad^{1,2}

¹SINTEF Materials and Chemistry, Applied Mechanics and Corrosion, Richard Birkelands vei 1C, NO-7465 Trondheim, Norway.

²Structural Impact Laboratory (SIMLab), Centre for Research-based Innovation, Norwegian University of Science and Technology, Richard Birkelands vei 1A, NO-7491 Trondheim, Norway.

³Norsk Hydro ASA, Research & Technology Development, Romsdalsvegen 4, NO-6600 Sunndalsøra, Norway.

⁴ Department for Structural Engineering, Norwegian University of Science and Technology, Richard Birkelands vei 1A, NO-7491 Trondheim, Norway.

In the previous ICAA event held in Aachen in 2008, a novel through-process modelling approach for prediction of the structural behaviour of high-pressure die-cast (HPDC) aluminium alloys was outlined. The approach included identification of critical defects in the castings, virtual reproduction of the defects in numerical casting simulations of mould filling and solidification, and mapping of these data onto a shell-based finite element (FE) mesh for subsequent structural simulations of generic HPDC components. The recent developments have been focused on dynamic effects and fracture propagation. The strain-rate sensitivity of Al die-cast materials has been investigated. Further, instrumented Charpy tests have been carried out to provide a database for the fracture and crack propagation behaviour under dynamic conditions. The experimental results are here compared to numerical predictions using brick elements.

Keywords: *mechanical properties, fracture, FE-analysis, through-process modelling, die-castings.*

1. Introduction

High-pressure die-casting (HPDC) aluminium alloys are of great importance for the automotive industry due to the potential for low weight, high production rate and the production of near net shape components of complex geometry. One market demand per se, is tailored high-pressure die-casting (HPDC) alloys with excellent castability and attractive mechanical properties in T1 condition being capable of self-piercing-riveting joining and welding to extruded aluminium alloys. The HPDC car components should withstand dynamic loading situations which require a fundamental interpretation of the controlling factors for sufficient deformation behaviour. Some defects, which are inherent to the HPDC process, affect the mechanical performance of die-castings. Macrosegregation of eutectic [1] and primary α -Al crystals [2], porosity [1], oxide bifilms and confluence welds [3] are addressed as typical HPDC defects. In this work, focus has been on the AlSi9MgMn alloy, both in T1 and T6 condition.

2. Experimental work

The strain-rate sensitivity was investigated experimentally by performing uniaxial tensile tests. Charpy tests were then performed to establish a database for the fracture and crack propagation behaviour under dynamic loading conditions.

2.1 Uniaxial tensile tests

Uniaxial tension test specimens were machined from cast plates (2.5 mm thickness) of the aluminium alloys AlSi9MgMn in T1 and T6 condition. A total of 32 specimens were tested under various loading conditions giving strain-rates in the range from 0.001 to 1 s⁻¹, i.e. 16 tests from each of the plates in T1 and T6 condition.

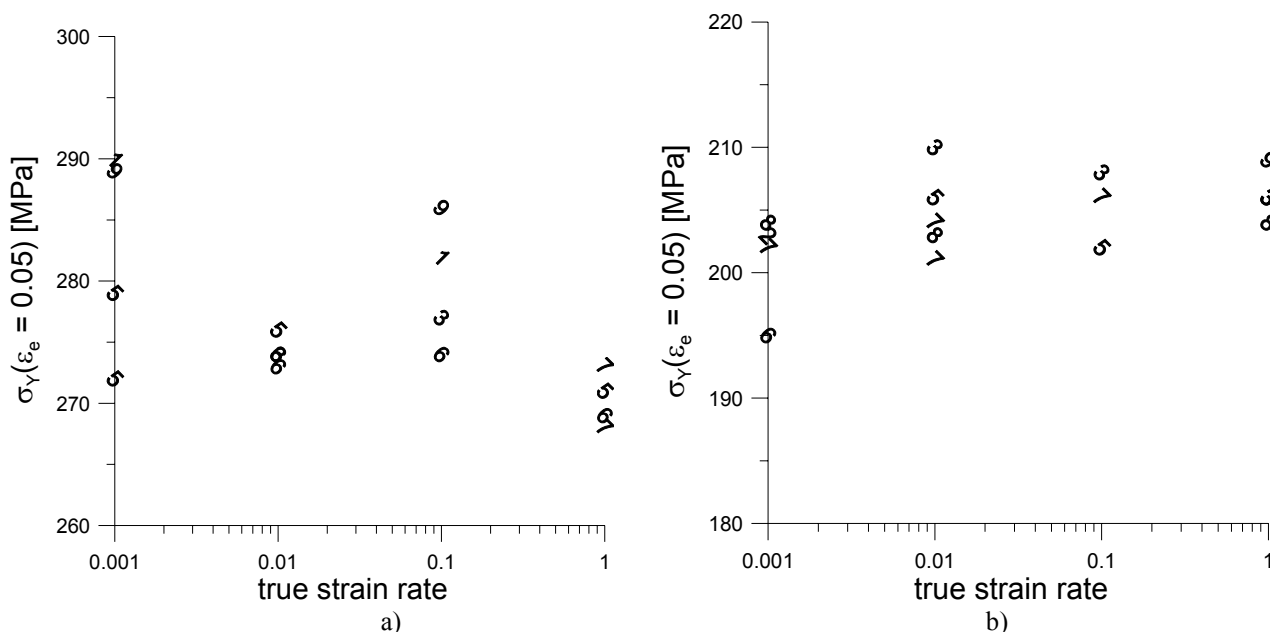


Fig. 1. Plots of the Cauchy stress at 0.05 equivalent plastic strain from uniaxial tests at different strain rates for a) AlSi9MgMn – T1 and b) AlSi9MgMn – T6.

Figure 1 shows plots of the Cauchy stress at 0.05 equivalent plastic strain from uniaxial tests at different strain rates for AlSi9MgMn in both T1 and T6 condition. The specimens were cut from several positions in the cast plates. These positions are symbolised with the numbers (1-9). The experimental data indicate that the strain-rate sensitivity is negligible for both tempers of the alloy.

Assuming rate-independent behaviour, the work hardening curves are represented in parametric form

$$\sigma_Y = \sigma_0 + \sum_{i=1}^2 Q_i (1 - \exp(-C_i \varepsilon_e)) \quad (1)$$

where σ_Y is the flow stress, ε_e is the equivalent plastic strain, σ_0 is the proportionality limit, and Q_i and C_i are hardening parameters. A least squares method was used to determine the parameters of this equation for each of the obtained work-hardening curves. It is noted that in uniaxial tension, the equivalent plastic strain equals the logarithmic plastic strain. The parameters of these mean curves are given in Table 1 for AlSi9MgMn in both T1 and T6 condition.

Table 1. Work hardening parameters.

Alloy	σ_0 [MPa]	Q_1 [MPa]	C_1	Q_2 [MPa]	C_2
AlSi9MgMn-T1	104.8	39.6	373.2	181.2	33.2
AlSi9MgMn-T6	96.9	60.2	80.1	87.6	11.4

2.2 Charpy tests

Figure 2 shows a schematic drawing of the instrumented Charpy V-notch impact test set-up, which consists of the specimen, the anvils, the striker equipped with wire resistance strain gauges, the striker arm and the body of the Charpy test machine. The striker has a mass of 21.1 kg. The impact

velocity of the striker is 5.52 m/s. The specimen is positioned upon two anvils with a span of 40 mm, and is broken by the impact of the heavy pendulum striker. The impact test device provides maximum impact energy of 320 J. The impact load is measured with strain gauges cemented on the tip of the striker. For each test, the force-displacement curve and energy-displacement curve are calculated from the measurements of force and time during impact. The specimen geometry is also provided in Figure 2. The total length of the specimen was 55 mm. The rectangular cross-section area was $10 \times 2.5 \text{ mm}^2$ for the test series considered here. The specimen had a 2 mm deep V-shaped notch with a flank angle of 45° . The notch tip radius is 0.25 mm. Figure 3 shows the recorded force-displacement characteristics from four Charpy tests of both AlSi9MgMn-T1, and AlSi9MgMn-T6. It is seen that the T1 material gives a higher force level during the test, but the ductility is significantly lower compared to the T6 material. The T6 material dissipates more energy compared to the T1 material.

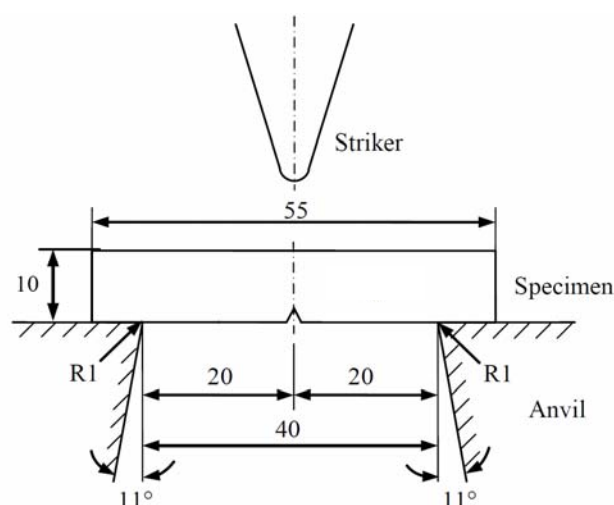


Fig. 2. Schematic drawing of the instrumented Charpy V-notch impact test set-up.

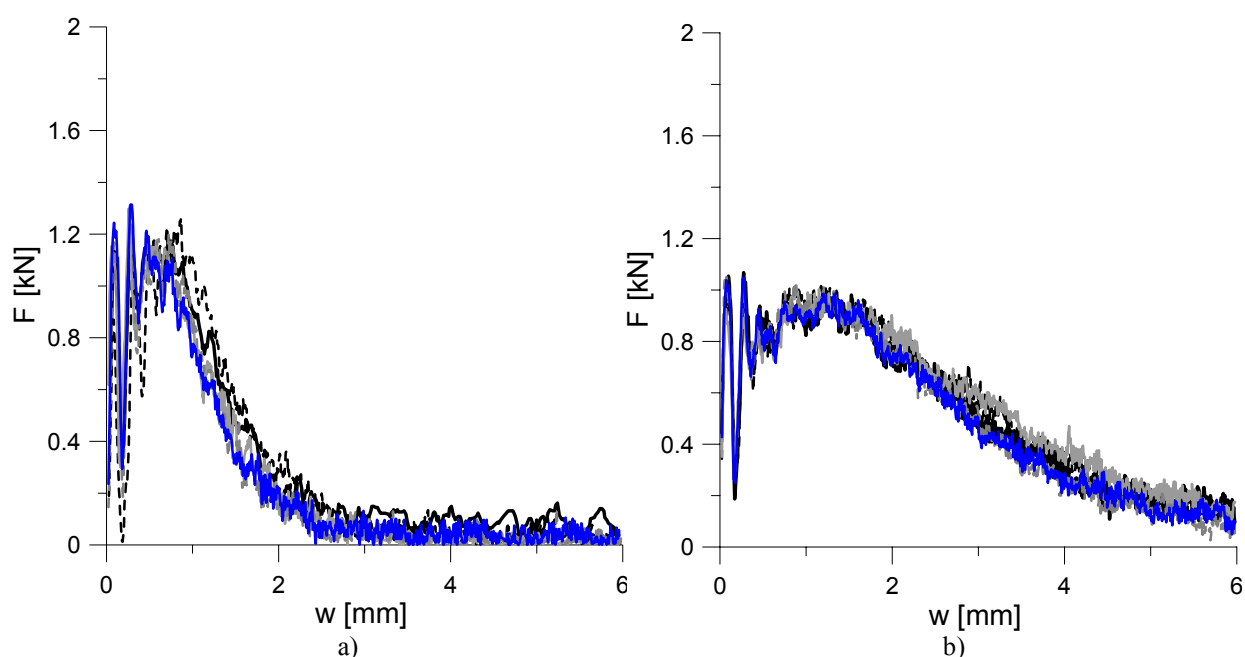


Fig. 3. Plots of the force-displacement measurements from Charpy tests of a) AlSi9MgMn-T1 and b) AlSi9MgMn-T6.

3. Through-process modelling concept

By making use of results from casting process simulations as quantitative measures for the position-dependent variations in mechanical properties of the cast material (e.g. outlet wall vs. inlet wall), a numerical through-process modelling approach for simulation of the structural performance of cast components can be established [4]:

- Simulation of the mould filling and solidification of the cast components.
- Mapping of results from casting process simulations to a FE model for simulation of the structural performance of the cast component, and establishment of a simplified quantitative correlation between results from the casting process simulation and experimentally measured values for the tensile ductility of the cast material.
- FE simulation of the cast components subjected to external loads (such as three-point bending tests or axial crushing). By using stochastic fracture parameters, the scatter in structural response can be predicted.

3.1 FE-based material and fracture modelling framework

The numerical calculations were carried out with a user-defined material model implemented in the commercial explicit FE-code LS-DYNA [5]: The material behaviour is described by the classical J_2 -flow theory, i.e. an elastic-plastic constitutive model including the von Mises yield criterion, the associated flow rule and isotropic hardening. Fracture is modelled by the Cockcroft-Latham criterion [6], assuming the fracture parameter to follow a modified weakest link Weibull distribution [7]. With this probabilistic fracture modelling approach, the fracture parameters can be introduced as stochastic parameters in the FE-simulations. More details about the implemented user-defined material model are given by Dørum et al. [8].

The yield function is defined by

$$f(\boldsymbol{\sigma}, \varepsilon_e) = \sigma_e(\boldsymbol{\sigma}) - \sigma_Y(\varepsilon_e) = 0 \quad (2)$$

where $\boldsymbol{\sigma}$ is the stress tensor, σ_e is the von Mises equivalent stress, and ε_e is the corresponding equivalent plastic strain. The flow stress σ_Y is defined by the isotropic hardening rule given by Eq. (1), and the corresponding work hardening parameters provided in Table 1. This implies that any variation in flow stress with position in the casting was not accounted for in the FE simulations. The Cockcroft-Latham fracture criterion reads

$$W = \int \max(\sigma_1, 0) d\varepsilon_e \leq W_c \quad (3)$$

where σ_1 is the maximum principal stress, and W_c is the value of the Cockcroft-Latham integral W giving fracture. This criterion implies that fracture is a function of the tensile stress σ_1 and equivalent plastic strain ε_e , and has the dimensions of work per unit volume. It is seen that fracture cannot occur when the maximum principal stress is compressive and that neither stresses nor strains alone are sufficient to cause fracture. Furthermore, the fracture strain increases with decreasing stress triaxiality and depends on the Lode parameter. As the Cockcroft-Latham fracture criterion is based upon only one parameter, a single material test is sufficient for the calibration.

The fracture parameter W_c of a finite element is assumed to follow a modified weakest-link Weibull distribution in the current study. The fracture probability of a material volume is given as

$$P(W) = 1 - \exp \left[- \left(\frac{V}{V_0} \right) \left(\frac{W}{W_{c0}} \right)^m \right] \quad (4)$$

where V is the volume of the element, V_0 is the scaling volume, W_{c0} is the scaling fracture parameter, and m is the Weibull modulus. It is seen that the probability of fracture increases with increasing volume V . Table 2 shows the parameters. It should be noted that these fracture parameters were extracted from quasi-static uniaxial tensile tests.

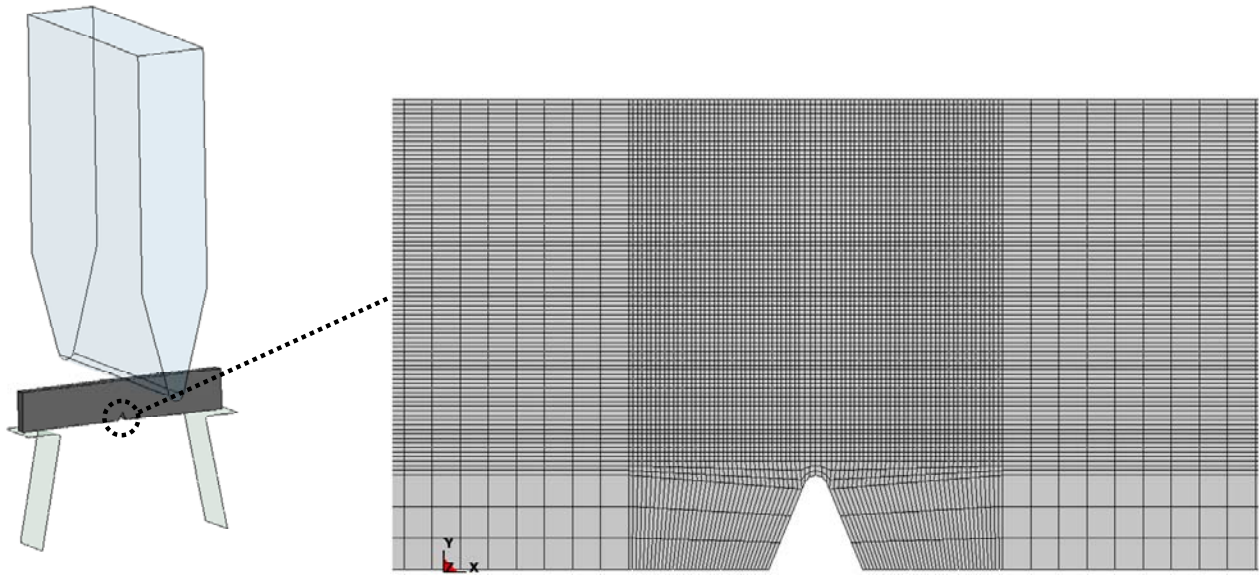


Fig. 4. FE model – 3D brick element mesh.

The Charpy test specimen was modelled with brick elements, and simulations were performed with different meshes with characteristic element lengths in the range 0.5-0.1 mm. An example of a FE model is given in Figure 4. The results showed that the crack propagation velocity decreases with increasing element size. Furthermore, with element lengths larger than 0.1 mm, the energy dissipation was overestimated. Figure 5 shows a comparison between the experimental and numerical simulations for AlSi9MgMn-T1 using a mesh with element lengths of approximately 0.1 mm. As noted in a work by Chen et al. [9], the numerical predictions are quite sensitive to friction. Here, simulations are carried out by assuming both frictionless contact and with friction coefficient equal to 0.4. It is seen that the latter gives the best correlation with respect to the experimental data. From the numerical simulations, it is seen that the maximum strain rate during fracture propagation is approximately 400 s^{-1} .

Table 2. Weibull parameters.

	V_0 [mm ²]	m	W_{c0} [MPa]	W_c^{\max} [MPa]
AlSi9MgMn – T1	320	3.06	16.0	58

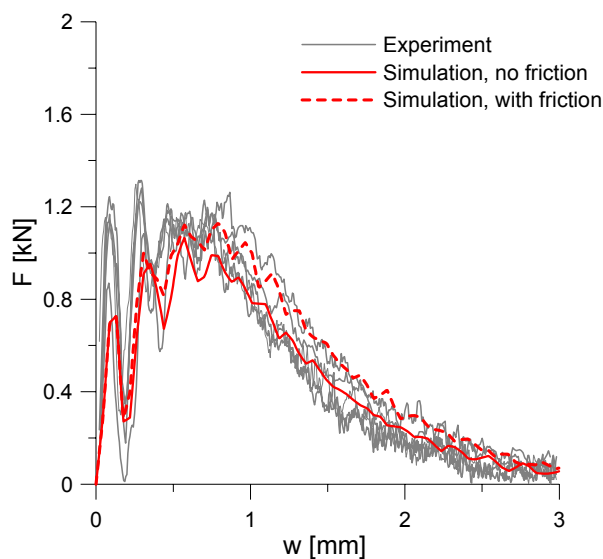


Fig. 5. Comparison between experimental and numerical simulations of the Charpy test for AlSi9MgMn-T1 using a mesh with element lengths of approximately 0.1 mm.

4. Concluding remarks

Strain-rate sensitivity studies were performed for the high pressure die-cast aluminium alloy AlSi9MgMn in T1 and T6 condition by performing uniaxial tensile tests at various loading velocities. The experimental data indicated that the strain-rate sensitivity is negligible. By performing Charpy tests, it was demonstrated that the increased ductility in the T6 heat-treated material gave a significant increase in the dissipated energy. Furthermore, numerical simulations of the Charpy test for AlSi9MgMn-T1, where the material parameters were calibrated on the basis of quasi-static material tests, gave good correlation with the experimental behaviour. Thus, the numerical simulations of the Charpy test support the assumption that strain-rate sensitivity can be neglected for the AlSi9MgMn alloy. However, it should be noted that the numerical simulations of the Charpy test are very dependent on the mesh size and the friction.

References

- [1] C.M. Gourlay, H.I. Laukli, A.K. Dahle, *Met. & Mat. Trans. A*, 2007, 38A, 1833-1844.
- [2] H.I. Laukli, C.M. Gourlay, A.K. Dahle, *Met. & Mat. Trans. A*, 2005, 36A, 805-818.
- [3] J. Campbell, *Materials Science & Technology*, 1988, 4, 194-204.
- [4] C. Dørum, H.I. Laukli, O.S. Hopperstad. Through-process numerical simulations of the structural behaviour of Al-Si die-castings. *Computational Materials Science* 46 (2009) 100–111. ISSN: 0927-0256.
- [5] LS-DYNA Keyword User's Manual, Version 971, Livermore Software Technology Corporation, May 2007.
- [6] M.G. Cockcroft, D.J. Latham. Ductility and the workability of metals, *J. Inst. Metals* 96, (1968) pp. 33-39.
- [7] W. Weibull. A statistical distribution function of wide applicability, *J. Appl. Mech.* 18 (1951), pp. 293-297.
- [8] C. Dørum, O.S. Hopperstad, T. Berstad, D. Dispinar. Numerical modelling of magnesium die-castings using stochastic fracture parameters. *Engineering Fracture Mechanics* 76 (2009) 2232–2248.
- [9] Y. Chen, O.S. Hopperstad, A.H. Clausen, T. Børvik, T. Berstad. Finite element analysis of Charpy tests on extruded aluminium alloys. 9th Int. DYMAT conference Sept. 2009, Belgium.